

1 **Evolution of host protease interactions among SARS-CoV-2 variants of concern and**  
2 **related coronaviruses**

3  
4 Edward R. Kastenhuber<sup>1</sup>, Jared L. Johnson<sup>1</sup>, Tomer M. Yaron<sup>1</sup>, Marisa Mercadante<sup>1</sup>, and Lewis  
5 C. Cantley<sup>1,2,\*</sup>

6  
7 Affiliations

8 1. Meyer Cancer Center, Department of Medicine, Weill Cornell Medical College, New York,  
9 NY, USA.

10 2. Dana Farber Cancer Institute, Boston, MA, USA.

11 \*Correspondence: [lcantley@med.cornell.edu](mailto:lcantley@med.cornell.edu)

12 **Abstract**

13 Previously, we showed that coagulation factors directly cleave SARS-CoV-2 spike and promote  
14 viral entry (Kasthuber et al., 2022). Here, we show that substitutions in the S1/S2 cleavage site  
15 observed in SARS-CoV-2 variants of concern (VOCs) exhibit divergent interactions with host  
16 proteases, including factor Xa and furin. Nafamostat remains effective to block coagulation factor-  
17 mediated cleavage of variant spike sequences. Furthermore, host protease usage has likely been a  
18 selection pressure throughout coronavirus evolution, and we observe convergence of distantly  
19 related coronaviruses to attain common host protease interactions, including coagulation factors.  
20 Interpretation of genomic surveillance of emerging SARS-CoV-2 variants and future zoonotic  
21 spillover is supported by functional characterization of recurrent emerging features.

22

23 **Keywords:**

24 SARS-CoV-2, COVID-19, coronavirus, variants, viral evolution, factor Xa, thrombin,  
25 coagulopathy

## 26 **Introduction**

27           The size and persistence of the viral reservoir in humans has driven considerable sequence  
28 variation among isolates of SARS-CoV-2 (Meredith et al., 2020), and distinct variant lineages  
29 have emerged (Konings et al., 2021; Kumar et al., 2021). The rapid rise and clonal expansion of  
30 the B.1.1.7 lineage (alpha variant), the B.1.617.2 lineage (delta variant), and subsequently, the  
31 B.1.1.529 lineage (omicron variant) suggest that some mutations have instilled variants with  
32 increased fitness (Harvey et al., 2021). Analysis of mutation accumulation and divergence  
33 indicates that changes in the spike S1 subunit are likely driver events in the outgrowth of emerging  
34 SARS-CoV-2 clades (Kistler et al., 2021).

35           The speed at which SARS-CoV-2 variants of concern have emerged has outpaced the rate  
36 at which researchers have been able to functionally characterize the effects of the mutations they  
37 harbor. The alpha, delta, and omicron variants exhibit enhanced fitness and/or escape from  
38 neutralizing antibodies, with respect to the ancestral wild type strain (Mlcochova et al., 2021;  
39 Planas et al., 2022; Shuai et al., 2022; Ulrich et al., 2022; Wang et al., 2021a). The SARS-CoV-2-  
40 S D614G substitution, which is common among VOCs, results in increased transmissibility via  
41 enhanced ACE2 binding and in hamster and ferret models (Hou et al., 2020; Korber et al., 2020;  
42 Plante et al., 2021; Zhou et al., 2021). Functional experiments have characterized the consequence  
43 of additional spike mutations on ACE2 binding (Starr et al., 2020) and escape from antibody  
44 neutralization (Chen et al., 2021; Greaney et al., 2021a; Greaney et al., 2021b; Starr et al., 2021;  
45 Wang et al., 2021b; Weisblum et al., 2020).

46           Coronaviruses, including SARS-CoV-2, typically require spike cleavage by host proteases  
47 at the S1/S2 boundary and S2' site to expose the fusion peptide and enable membrane fusion and  
48 viral entry (Belouzard et al., 2009; Glowacka et al., 2011; Hoffmann et al., 2020a; Jaimes et al.,  
49 2020a; Jaimes et al., 2020c; Millet and Whittaker, 2014; Walls et al., 2020). The mechanism of  
50 cleavage activation of spike by host proteases is conserved across coronaviruses, but the cleavage  
51 recognition site is not conserved (Jaimes et al., 2020b). Viral interaction with host proteases poses  
52 a significant barrier for zoonotic spillover (Letko et al., 2020; Menachery et al., 2020) and a  
53 potential target for antiviral drugs (Hoffmann *et al.*, 2020a; Hoffmann et al., 2020b). One of the  
54 most dynamic loci in the emerging lineages of SARS-CoV-2 is the S1/S2 spike cleavage site.  
55 Specifically, the P5 position, five amino acids to the N-terminal of the cleaved peptide bond, has  
56 been highly variable in the population of SARS-CoV-2. This position is subject to P681H

57 substitution in the B.1.1.7 lineage (alpha variant) and the B.1.1.529 lineage (omicron variant);  
58 P681R substitution is present in the B.1.617.2 lineage (delta variant).

59 We recently discovered that coagulation factors can cleave and activate SARS-CoV-2  
60 spike, enhancing viral entry into cells (Kasthuber *et al.*, 2022). Herein, we use FRET-based  
61 enzymatic assays to investigate the effects of mutations in SARS-CoV-2 variants of concern on  
62 interaction with factor Xa and other host proteases. Furthermore, we explored how spike cleavage  
63 sites in distantly related coronaviruses interact with various host proteases.

## 64 **Results**

### 65 *Sequence divergence of SARS-CoV-2 spike codon 681 among variants of concern*

66 Up to this point, spike codon 681, which resides in the S1/S2 cleavage site (**Fig. 1A**), is  
67 one of the highest entropy sites in the SARS-CoV-2 genome among sequenced samples (Elbe and  
68 Buckland-Merrett, 2017; Hadfield et al., 2018; Sagulenko et al., 2018). Beginning in December  
69 2019, viral genomes have been collected globally and made available by GISAID and Nextstrain  
70 (<https://nextstrain.org/>), of which we visualized a subsample (Elbe and Buckland-Merrett, 2017;  
71 Hadfield *et al.*, 2018). For nearly a year, SARS-CoV-2 spike encoded for proline at position 681  
72 in almost all isolates. Samples with P681H substitution emerged in October 2020 and surpassed  
73 the frequency of P681 by March 2021 (**Fig. 1A**). Meanwhile, a P681R substitution emerged within  
74 the B.1.617.2 lineage (delta variant), and rapidly became predominant by June 2021 (**Fig. 1A**).  
75 Subsequently, the P681H substitution once again became prevalent during the clonal sweep of the  
76 Omicron variant. (**Fig. 1A**).

77 The P681H substitution is one of many defining mutations of the B.1.1.7 lineage (alpha  
78 variant) and the P681R substitution is one of many defining mutations of the B.1.617.2 lineage  
79 (delta variant). Numerous factors may have contributed the rise in frequency of these mutations,  
80 including positive selection of other driver mutations co-occurring in the same lineage, and  
81 representation of different regions in deposited viral genomes. However, outside of the primary  
82 clades, both P681H and P681R appear to have arisen independently multiple times and shown  
83 evidence of expansion through transmission, consistent with the possibility of a functional  
84 advantage (**Fig. 1B**).

85

### 86 *Substitutions at SARS-CoV-2 Spike S1/S2 site cause divergent changes to interactions with host* 87 *proteases*

88 We specifically tested how substitutions observed in emerging lineages of SARS-CoV-2  
89 variants affect cleavage of the spike S1/S2 site by various host proteases. Comparing enzyme  
90 kinetics on peptide substrates with P681 (WT, corresponding to Wuhan-Hu1) and B.1.1.7  
91 (P681H), we found that the P681H led to an increase in factor Xa activity (**Fig. 2A**), but we found  
92 no evidence for changes in cleavability by furin, TMPRSS2, or thrombin (**Fig. 2B-D**). On the other  
93 hand, P681R substitution increased  $V_{\max}$  of factor Xa by 65% as well as increasing  $V_{\max}$  of furin

94 cleavage by 99% with respect to the ancestral WT sequence (**Fig. 2A-B**). TMPRSS2 and thrombin  
95 showed decreased activity against the P681R substrate (**Fig. 2C-D**).

96

97 *SARS-CoV-2 spike variants remain sensitive to nafamostat*

98 Nafamostat was found to be a multi-targeted inhibitor of TMPRSS2 as well as coagulation  
99 factors and other transmembrane serine proteases involved in viral entry (Kasthuber *et al.*,  
100 2022). We investigated whether mutations in the S1/S2 site could affect the efficacy of nafamostat  
101 to block factor Xa-mediated spike cleavage. Although factor Xa exhibits increased  $V_{max}$  with  
102 P681H and P681R variant substrates (**Fig. 2A**), factor Xa cleavage of both variant substrates  
103 remains equivalently sensitive to nafamostat (**Fig. 3A-C**).

104

105 *Effect of phosphorylation at the S1/S2 site on spike cleavage*

106 We hypothesized that interaction with host kinases could modify interactions with host  
107 proteases. To evaluate how phosphorylation at serine residues near the S1/S2 site influence the  
108 cleavability of the site by proteases, we used singly phosphorylated peptide substrates  
109 corresponding to the S680, S686, and S689 residues (**Fig. 4A**). Phosphorylation of Ser 680, in the  
110 P6 position upstream of the cleavage site, completely abolished furin cleavage and had a moderate  
111 impact (30-50% inhibition) on factor Xa, TMPRSS2, and thrombin cleavage (**Fig. 4B-E**).  
112 Phosphorylation of Ser 686, in the P-1 position immediately adjacent to the cleaved amide bond,  
113 had a strong inhibitory effect on all four proteases (**Fig. 4B-E**). Phosphorylation of Ser 689, in the  
114 P-4 position C-terminal to the cleavage site, had enzyme-specific effects on cleavage. Factor Xa  
115 and TMPRSS2 were moderately inhibited and thrombin was strongly inhibited by p-S689 (**Fig.**  
116 **4B,D,E**); however, furin cleavage was enhanced by p-S689 (**Fig. 4C**). Post-translational  
117 modification by phosphorylation has substantial effects on the cleavability of the S1/S2 site.

118

119 *Convergent evolution of cleavability by host proteases in diverse coronavirus species*

120 It is not clear to what extent the cleavability by coagulation factors is specific to SARS-  
121 CoV-2 and its variants or if this is a common feature among coronaviruses. The coronaviridae  
122 family is categorized into four genera (alphacoronavirus, betacoronavirus, gammacoronavirus, and  
123 deltacoronavirus) with differences in sequence, function, and host range (Cui *et al.*, 2019).  
124 Betacoronaviruses have evolved into four divergent lineages A-D, where lineage A contains

125 common cold coronavirus HCoV-OC43, lineage B contains SARS and SARS-CoV-2, and lineage  
126 C contains MERS (Jaimes *et al.*, 2020b) (**Fig. 4A**). We examined the interactions between host  
127 proteases and peptide substrates corresponding to a variety of betacoronaviruses from different  
128 lineages, and an outgroup avian gammacoronavirus infectious bronchitis virus (IBV-Beaudette).  
129 These substrates included diverse coronaviruses, severe and mild, zoonic and host-restricted.  
130 Interestingly, we found that no two species of coronavirus had identical susceptibility to host  
131 proteases. Only the SARS-CoV-2 S1/S2 site is cleavable by all four enzymes studied (**Fig. 4B-C**,  
132 **E**). In addition to SARS-CoV-2 S1/S2, factor Xa showed remarkable activity against HCoV-OC43  
133 S1/S2 (**Fig. 4B**). A sequence from a clinical isolate of HCoV-OC43 (S1/S2-OC43/Seattle), but not  
134 the mouse-passaged laboratory strain of HCoV-OC43 (S1/S2-OC43/ATCC) was furin-sensitive  
135 (**Fig. 4B**). Furin efficiently cleaved both the S1/S2 and the S2' sites of IBV-Beaudette, although  
136 these substrates were not preferred by the other enzymes tested (**Fig. 4B**). Cleavability by thrombin  
137 was observed for the S1/S2 sites of SARS, MERS, and SARS-CoV-2, but not RatG13, a bat  
138 coronavirus with the highest known genome-wide sequence identity to SARS-CoV-2 (**Fig. 4C**).  
139 TMPRSS2 showed, on average, relatively low activity, but was active against a wider variety of  
140 both S1/S2 and S2' substrates in the coronavirus substrate panel (**Fig. 4D**). While each coronavirus  
141 examined has a distinct set of interactions with host proteases, common solutions have been  
142 reached by distantly related viruses, suggesting convergent evolution.

143 **Discussion**

144 *SARS-CoV-2 variants of concern exhibit divergent interactions with host proteases*

145 Substitutions within the spike protease cleavage sites of SARS-CoV-2 VOCs modify viral  
146 interaction with host proteases. Spike substitution P681R increases furin cleavability, while P681H  
147 does not, in agreement with previous reports (Liu et al., 2021; Lubinski et al., 2021a; Lubinski et  
148 al., 2021b). A simplified model of SARS-CoV-2 spike activation is that furin cleaves the S1/S2  
149 site, which potentiates either TMPRSS2 cleavage at the S2' site or cleavage by endosomal  
150 cathepsin L at an undetermined alternative site (Bestle et al., 2020; Hoffmann *et al.*, 2020a; Jaimes  
151 *et al.*, 2020a; Ou et al., 2020). However, additional host proteases including other TTSPs and  
152 coagulation factors can substitute or augment these steps (Kastenhuber *et al.*, 2022; Tang et al.,  
153 2021). Given that recurrent substitutions at P681 (adjacent to the S1/S2 site) have divergent effects  
154 on furin cleavage, it is likely that modified interaction with other host proteins likely contribute to  
155 selection pressure on the sequence of the S1/S2 site. For example, both P681H and P681R  
156 substitutions increase susceptibility to factor Xa-mediated cleavage. The effect of factor Xa can  
157 easily be overlooked as it is not apparent in the setting of cell culture or organoid experiments,  
158 unless added exogenously. Also, animal models of coronavirus have not been described to  
159 recapitulate coagulopathy associated with severe disease in humans (Kim et al., 2020; Leist et al.,  
160 2020; Sia et al., 2020; Zheng et al., 2021). The role of coagulation factors and other  
161 microenvironmentally-derived proteases merit further study among emerging viral variants.

162

163 *Functional characterization to support interpretation of emerging VOCs and zoonotic spillover*  
164 *events.*

165 The COVID-19 pandemic is an extremely challenging global health crisis, exacerbated by  
166 the continued emergence of viral variants, the impact of which can often only be seen posteriorly.  
167 Furthermore, the zoonotic spillover of SARS, MERS, and SARS-CoV-2 within the last 20 years  
168 has caused concern for additional novel coronavirus epidemics in the future. Conditions associated  
169 with heightened risk of zoonotic transmission of novel viruses include changes in the extent of  
170 human contact with wildlife and livestock, increasing urbanization and travel, and an accelerating  
171 rate of interspecies “first contacts” due to climate-induced migration (Carlson et al., 2022).  
172 Genomic surveillance is a critical tool for tracking emerging variants of SARS-CoV-2 and threats  
173 of novel species of coronavirus from other mammalian hosts (Walensky et al., 2021). However, it



174 can be difficult to extrapolate phenotypic consequences from genomic sequence alone and  
175 fluctuations in variant prevalence can be driven by local changes in human behavior and public  
176 health policy as well as characteristics of the viral variant. The B.1.1.7 lineage (alpha variant), the  
177 B.1.617.2 lineage (delta variant), and the B.1.1.529 lineage (omicron variant) have undergone near  
178 clonal sweeps of the population of SARS-CoV-2 in humans. For unclear reasons, the P.1 (gamma  
179 variant) and B.1.526 (iota variant) lineages have faded and been displaced after their initial  
180 emergence and expansion (Annavajhala et al., 2021). Fitness advantage can be mediated by a  
181 variety of specific functional phenotypes including transmission efficiency, viral particle stability,  
182 infection cycle time, immune escape, and disease severity (Mlcochova et al., 2021; Wang et al.,  
183 2021a). The goal of functional characterization of recurrently mutated sites is to anticipate the  
184 impact of novel variants of concern and the utility of available interventions.

185

#### 186 *Towards broad coronavirus antiviral drugs*

187 In the first two years of the COVID-19 pandemic, vaccines and nonpharmaceutical  
188 interventions have saved many lives (McNamara et al., 2022; Mesle et al., 2021; Victora et al.,  
189 2021). Anticipating the continued evolution of SARS-CoV-2 variants and future zoonotic spillover  
190 transmission of novel coronaviruses, the development of broad-acting antivirals is an area of great  
191 interest. Coronavirus antiviral development has thus far targeted viral RdRp (Remdesivir) and  
192 viral protease Mpro (Paxlovid) (Beigel et al., 2020; Hammond et al., 2022). Host-targeted  
193 antivirals, including repurposed (Hoffmann et al., 2020a; Hoffmann et al., 2020b) and novel  
194 TMPRSS2 inhibitors (Shapira et al., 2022), have been shown to reduce viral entry. We previously  
195 demonstrated that nafamostat also inhibits both TMPRSS2 and coagulation factors, which may be  
196 a collateral benefit in anti-coronavirus activity (Kastenhuber et al., 2022). Although variations in  
197 the S1/S2 site sequence have resulted in enhanced factor Xa cleavability, we show here that  
198 nafamostat remains effective to block FXa-mediated cleavage of variant S1/S2 sites. Nafamostat  
199 also exhibits antiviral activity against human coronaviruses 229E and NL6, associated with milder  
200 seasonal illness (Niemeyer et al., 2021). Early, outpatient intervention with orally available drugs  
201 would be advantageous (Griffin et al., 2021), but nafamostat is an intravenous drug with a  
202 suboptimal PK profile (Quinn et al., 2022). On the other hand, intranasal delivery of nafamostat  
203 was effective in mouse models of COVID-19 and may be a promising approach (Li et al., 2021).

204 Development of novel drugs with activity against relevant host proteases could be a valuable  
205 advancement for broad coronavirus antivirals.

206

### 207 *Phospho-regulation of SARS-CoV-2 spike cleavage*

208 We found that phosphorylation of the S1/S2 site generally reduces cleavability by factor  
209 Xa, furin, TMPRSS2, and thrombin. It is understandable that a region that favors multiple basic  
210 residues for function would be inhibited by negative charge associated with phosphorylation.  
211 Phosphorylation of S680 and S686 have previously been described to inhibit furin cleavage (Ord  
212 et al., 2020). While phosphoproteomics analysis of SARS-CoV-2 viral proteins revealed numerous  
213 phosphorylation events throughout the viral proteome, no phosphorylated serine residues near the  
214 S1/S2 site have been detected (Bouhaddou et al., 2020; Davidson et al., 2020; Hekman et al., 2020;  
215 Klann et al., 2020; Stukalov et al., 2021; Yaron et al., 2020). The lack of observed phosphorylation  
216 and the robustness of SARS-CoV-2 replication would suggest that inhibitory phospho-regulation  
217 is not effective in infected cells. One might predict that selection pressure on the S1/S2 site  
218 disfavors host kinase substrate motifs so as to avoid inhibitory phosphorylation, but this does not  
219 necessarily appear to be the case (Ord *et al.*, 2020)(data not shown). Alternatively, negative  
220 selection pressure through host kinase interaction could be avoided by subcellular  
221 compartmentalization of viral biogenesis, interference by other PTMs adjacent residues (including  
222 glycosylation), or exposure to host phosphatases. It is also plausible that lineage-specific  
223 expression of kinases capable of suppressing proteolytic processing of the spike could contribute  
224 to cellular tropism of SARS-CoV-2.

225

### 226 *Convergent evolution of host protease interactions among diverse coronavirus species*

227 Proteolysis of coronavirus spike proteins by host proteases is clearly a selection pressure  
228 and a barrier to zoonotic spillover (Menachery *et al.*, 2020). Coronavirus S1/S2 and S2' cleavage  
229 sites exhibit distinct proteolytic fingerprints, which highlights the nuanced substrate recognition  
230 of human trypsin-like serine proteases, beyond the preference for arginine at the P1 position of the  
231 substrate (Goettig et al., 2019). The human genome encodes for more than 500 proteases and many  
232 proteases have not been sufficiently profiled to predict *in silico* which proteases are capable of  
233 cleaving a given viral sequence with any degree of certainty (Puente et al., 2005; Rawlings et al.,  
234 2018), obviating the need for direct biochemical evidence of viral interactions with host proteases.

235 Distantly related species of coronavirus have acquired the capacity to interact with  
236 overlapping collections of host proteases. This would suggest that selection pressure for host-  
237 mediated cleavage activation has led to convergent solutions of this critical function in multiple,  
238 independent evolutionary events. Sequence analysis has shown that furin cleavage motifs  
239 containing RXXR can be found in multiple genera of coronavirus, including a variety of  
240 betacoronaviruses (Wu and Zhao, 2020). Our data functionally confirm that furin cleavage sites,  
241 and cleavage sites of other host proteases, are widely distributed throughout coronavirus  
242 phylogeny, supporting the notion that novel protease sites emerge regularly in the evolution of  
243 coronaviruses. There has been speculation that the insertion of a polybasic sequence at the S1/S2  
244 site of SARS-CoV-2 is suggestive of laboratory manipulation (Maxmen and Mallapaty, 2021), but  
245 this relies on the implicit assumptions that the inserted PRRA sequence has been optimized for  
246 propagation in humans and that a protease cleavage site is unlikely to emerge during natural  
247 selection. Instead, the S1/S2 site has been one of the sites in the SARS-CoV-2 genome harboring  
248 the most variation after the virus has propagated in the human population and selection for novel  
249 protease sites is a core feature of coronavirus evolution. Expanding the mechanistic depth of  
250 coronavirus host protease usage is critical to understanding coronavirus pathogenesis, to fully take  
251 advantage of genomic surveillance, and to develop pan-coronavirus antivirals.

252 **Author Contributions**

253 Conceptualization, E.R.K and L.C.C.; Methodology, E.R.K, J.L.J., T.M.Y.; Investigation, E.R.K.  
254 and M.M; Writing – Original Draft, E.R.K.; Writing – Review & Editing, E.R.K. and L.C.C.;  
255 Resources, J.L.J., T.M.Y.; Funding Acquisition, L.C.C.; Supervision, L.C.C..

256

257 **Acknowledgements**

258 The authors would like to thank Gary R. Whittaker (Cornell University), Robert E. Schwartz  
259 (WCMC), and all members of the Cantley Lab for insightful discussion and helpful comments.  
260 The efforts of the Nextstrain team and contributors to GISAID were invaluable to this study. This  
261 work was funded in part by the National Institute of Health research grant R35 CA197588 (to  
262 LCC) and the Pershing Square Foundation (L.C.C.).

263

264 **Declarations of Interests**

265 LCC is a founder and member of the SAB of Agios Pharmaceuticals and a founder and former  
266 member of the SAB of Ravenna Pharmaceuticals (previously Petra Pharmaceuticals). These  
267 companies are developing novel therapies for cancer. LCC holds equity in Agios. LCC's  
268 laboratory also received some financial support from Ravenna Pharmaceuticals. T.M.Y. is a  
269 stockholder and on the board of directors of DESTROKE, Inc., an early-stage start-up developing  
270 mobile technology for automated clinical stroke detection.

271

272 **Figure Legends**

273 **Figure 1. Sequence divergence of SARS-CoV-2 spike-681 among variants of concern. (A)**

274 Schematic of SARS-CoV-2 spike protein, highlighting position 681 adjacent to the S1/S2 site.

275 Modified from (Kasthuber *et al.*, 2022). A subsampled collection of 3043 samples from

276 between Dec 2109 and May 2022 from GISAID was obtained and visualized using Nextstrain

277 (<https://nextstrain.org/ncov>) (Elbe and Buckland-Merrett, 2017; Hadfield *et al.*, 2018). **(B)**

278 Frequency of viral genomes sequenced with proline (black), histidine (red), or arginine (blue) at

279 spike codon 681 by date of sample collection. **(C)** Phylogenetic tree rendered by Nextstrain.

280 Genotype at S681 of each sample is indicated by proline (gray), histidine (red), or arginine

281 (blue). Branches corresponding to dominant variants of concern are highlighted in the outer ring.

282

283 **Figure 2. Substitutions at SARS-CoV-2 Spike S1/S2 site cause divergent changes to**

284 **interactions with host proteases.** Reaction rates (expressed as initial reaction velocity  $V_0$

285 normalized to the concentration of enzyme  $E_i$ ) for the cleavage of SARS-CoV-2 spike S1/S2

286 ancestral (P681) and variant (P681H and P681R) peptide substrates by **(A)** factor Xa, **(B)** furin,

287 and **(C)** TMPRSS2, and **(D)** Thrombin were measured over a range of 0-80  $\mu$ M substrate.

288

289 **Figure 3. SARS-CoV-2 spike variants remain sensitive to nafamostat.** Relative activity of

290 factor Xa (125nM) with or without 10 $\mu$ M nafamostat in reaction with S1/S2 FRET peptide

291 substrate (50  $\mu$ M) corresponding to **(A)** WT ancestral sequence P681, **(B)** P681H substitution,

292 and **(C)** P681R substitution. \*  $P < 0.05$ , two-tailed t-test. Error bars represent +/- SEM.

293

294 **Figure 4. Effect of phosphorylation at the S1/S2 site on spike cleavage. (A)** Phosphorylated

295 peptides were generated for serine residues (S680, S686, S689). Reaction rates (expressed as

296 initial reaction velocity  $V_0$  normalized to the concentration of enzyme  $E_t$ ) for the cleavage of

297 unmodified or phosphorylated substrates by **(B)** factor Xa, **(C)** furin, and **(D)** TMPRSS2, and **(E)**

298 Thrombin were measured over a range of 0-80  $\mu$ M substrate.

299

300 **Figure 5. Proteolytic fingerprint of diverse coronavirus lineages. (A)** Phylogenic relationship  
301 of a panel of coronaviruses with the corresponding aligned S1/S2 and S2' cleavage sites.  
302 Heatmaps depicting the initial velocity  $V_0$  of cleavage of the indicated peptide substrates (rows)  
303 and concentrations (columns) by **(B)** factor Xa, **(C)** furin, **(D)** TMPRSS2, and **(E)** thrombin.

304 **Methods**

Key Resources Table				
Reagent type (species) or resource	Designation	Source or reference	Identifiers	Additional information
chemical compound, drug	Nafamostat	Selleck	Cat# S1386	
peptide, recombinant protein	Thrombin	Millipore Sigma	Cat# 605195	
peptide, recombinant protein	Factor Xa	Millipore Sigma	Cat# 69036	
peptide, recombinant protein	TMPRSS2	LSBio	Cat# LS-G57269	
peptide, recombinant protein	Furin	Thermo Fisher Scientific	Cat# 1503SE010	
peptide, recombinant protein	SARS-CoV-2-S1/S2-P681	Anaspec	SARSCoV-2-Wuhan-Hu1 (MN908947.3)	QXL520-SPRRARSVA SQ-K(5-FAM)-NH2
peptide, recombinant protein	SARS-CoV-2-S1/S2-P681H	Anaspec		QXL520-SHRRARSV ASQ-K(5-FAM)-NH2
peptide, recombinant protein	SARS-CoV-2-S1/S2-P681R	Anaspec		QXL520-SRRRARSV ASQ-K(5-FAM)-NH2
peptide, recombinant protein	SARS-CoV-2-S2p	Anaspec	SARSCoV-2-Wuhan-Hu1 (MN908947.3)	QXL520-KPSKRSEFIE D-K(5-FAM)-NH2

peptide, recombinant protein	S1/S2-OC43/ATCC	Anaspec		QXL520-KNRRSRGAI TT-K(5-FAM)-NH2
peptide, recombinant protein	S1/S2-OC43/Seattle	Anaspec	HCoV-OC43 (KF963244.1)	QXL520-KNRRSRAI TT-K(5-FAM)-NH2
peptide, recombinant protein	S1/S2-SARS	Anaspec	hSARS-CoV-Tor2 (NC_004718.3)	QXL520-TVSLLRSTS QK-K(5-FAM)-NH2
peptide, recombinant protein	S1/S2-RaTG13	Anaspec	BatSL-RaTG13 (EPI_ISL_402131)	QXL520-TQTNSRSVA SQ-K(5-FAM)-NH2
peptide, recombinant protein	S1/S2-Bat-SL-CoV-ZC45	Anaspec	Bat-SL-CoVZC45 (MG772933.1)	QXL520-TASILRSTS QK-K(5-FAM)-NH2
peptide, recombinant protein	S1/S2-MERS	Anaspec	MERS-CoV-Jordan-N3 (KC776174.1)	QXL520-TPRSVRSVP GE -K(5-FAM)-NH2
peptide, recombinant protein	S1/S2-IBV-Beaudette	Anaspec		QXL520-TRRFRRSIT EN-K(5-FAM)-NH2
peptide, recombinant protein	S2p-OC43	Anaspec	HCoV-OC43 (KF963244.1)	QXL520-SKASSRSAI ED-K(5-FAM)-NH2
peptide, recombinant protein	S2p-SARS	Anaspec	hSARS-CoV-Tor2	QXL520-LKPTKRSFIE D-K(5-FAM)-NH2



			(NC_004718.3)	
peptide, recombinant protein	S2p-MERS	Anaspec	MERS-CoV-Jordan-N3 (KC776174.1)	QXL520-GSRSARSAI ED-K(5-FAM)-NH2
peptide, recombinant protein	S2p-IBV-Beaudette	Anaspec		QXL520-SSRRKRSLI ED-K(5-FAM)-NH2
software, algorithm	Prism 9	GraphPad Software		

305

### 306 **Sequence Analysis**

307 A subsampled collection of 3043 samples from between Dec 2109 and May 2022 from GISAID  
308 was obtained and visualized using Nextstrain on June 3, 2022  
309 ([https://nextstrain.org/ncov/gisaid/global/all-time?c=gt-S\\_681&l=radial](https://nextstrain.org/ncov/gisaid/global/all-time?c=gt-S_681&l=radial)) (Elbe and Buckland-  
310 Merrett, 2017; Hadfield *et al.*, 2018). Dataset parameters were set to ncov, gisaid, global, all-  
311 time. Sample clades and phylogeny were defined using default settings of Nextstrain and  
312 displayed in radial mode.

313

### 314 **Enzymatic Assay**

315 Thrombin (605195) and Factor Xa, activated by Russell's Viper Venom, were obtained from  
316 Millipore Sigma (69036). TMPRSS2, purified from yeast, was obtained from LSBio (LS-  
317 G57269). Furin was obtained from Thermo Fisher Scientific (1503SE010). FRET peptides were  
318 obtained from Anaspec and all peptide sequences are listed in the **Key resources table**. Protease  
319 assay buffer was composed of 50mM Tris-HCl, 150mM NaCl, pH 8. Enzyme dilution/storage  
320 buffer was 20mM Tris-HCl, 500mM NaCl, 2mM CaCl<sub>2</sub>, 50% glycerol, pH 8. Peptides were  
321 reconstituted and diluted in DMSO. Furin was used at a final concentration of 30 nM and all other  
322 enzymes were used at a final concentration of 125nM. Enzyme kinetics were assayed in black 96W  
323 plates with clear bottom and measured using a BMG Labtech FLUOstar Omega plate reader,

324 reading fluorescence (excitation 485nm, emission 520nm) every minute for 20 cycles, followed  
325 by every 5 minutes for an additional 8 cycles. A standard curve of 5-FAM from 0-10  $\mu$ M (1:2  
326 serial dilutions) was used to convert RFU to  $\mu$ M of cleaved FRET peptide product. Calculation of  
327 enzyme constants was performed with Graphpad Prism software (version 9.0). Nafamostat was  
328 obtained from Selleck Chemicals.

329  
330  
331  
332  
333  
334  
335  
336  
337  
338  
339  
340  
341  
342  
343  
344  
345  
346  
347  
348  
349  
350  
351  
352  
353  
354  
355  
356  
357  
358  
359  
360  
361  
362  
363  
364  
365  
366  
367  
368  
369  
370  
371  
372  
373  
374  
375  
376  
377

References:

Annavajhala, M.K., Mohri, H., Wang, P., Nair, M., Zucker, J.E., Sheng, Z., Gomez-Simmonds, A., Kelley, A.L., Tagliavia, M., Huang, Y., et al. (2021). Emergence and expansion of SARS-CoV-2 B.1.526 after identification in New York. *Nature* *597*, 703-708. [10.1038/s41586-021-03908-2](https://doi.org/10.1038/s41586-021-03908-2).

Beigel, J.H., Tomashek, K.M., Dodd, L.E., Mehta, A.K., Zingman, B.S., Kalil, A.C., Hohmann, E., Chu, H.Y., Luetkemeyer, A., Kline, S., et al. (2020). Remdesivir for the Treatment of Covid-19 - Final Report. *N Engl J Med* *383*, 1813-1826. [10.1056/NEJMoa2007764](https://doi.org/10.1056/NEJMoa2007764).

Belouzard, S., Chu, V.C., and Whittaker, G.R. (2009). Activation of the SARS coronavirus spike protein via sequential proteolytic cleavage at two distinct sites. *Proc Natl Acad Sci U S A* *106*, 5871-5876. [10.1073/pnas.0809524106](https://doi.org/10.1073/pnas.0809524106).

Bestle, D., Heindl, M.R., Limburg, H., Van Lam van, T., Pilgram, O., Moulton, H., Stein, D.A., Harges, K., Eickmann, M., Dolnik, O., et al. (2020). TMPRSS2 and furin are both essential for proteolytic activation of SARS-CoV-2 in human airway cells. *Life Sci Alliance* *3*. [10.26508/lsa.202000786](https://doi.org/10.26508/lsa.202000786).

Bouhaddou, M., Memon, D., Meyer, B., White, K.M., Rezelj, V.V., Correa Marrero, M., Polacco, B.J., Melnyk, J.E., Ulferts, S., Kaake, R.M., et al. (2020). The Global Phosphorylation Landscape of SARS-CoV-2 Infection. *Cell* *182*, 685-712 e619. [10.1016/j.cell.2020.06.034](https://doi.org/10.1016/j.cell.2020.06.034).

Carlson, C.J., Albery, G.F., Merow, C., Trisos, C.H., Zipfel, C.M., Eskew, E.A., Olival, K.J., Ross, N., and Bansal, S. (2022). Climate change increases cross-species viral transmission risk. *Nature*. [10.1038/s41586-022-04788-w](https://doi.org/10.1038/s41586-022-04788-w).

Chen, R.E., Zhang, X., Case, J.B., Winkler, E.S., Liu, Y., VanBlargan, L.A., Liu, J., Errico, J.M., Xie, X., Suryadevara, N., et al. (2021). Resistance of SARS-CoV-2 variants to neutralization by monoclonal and serum-derived polyclonal antibodies. *Nat Med* *27*, 717-726. [10.1038/s41591-021-01294-w](https://doi.org/10.1038/s41591-021-01294-w).

Cui, J., Li, F., and Shi, Z.L. (2019). Origin and evolution of pathogenic coronaviruses. *Nat Rev Microbiol* *17*, 181-192. [10.1038/s41579-018-0118-9](https://doi.org/10.1038/s41579-018-0118-9).

Davidson, A.D., Williamson, M.K., Lewis, S., Shoemark, D., Carroll, M.W., Heesom, K.J., Zambon, M., Ellis, J., Lewis, P.A., Hiscox, J.A., and Matthews, D.A. (2020). Characterisation of the transcriptome and proteome of SARS-CoV-2 reveals a cell passage induced in-frame deletion of the furin-like cleavage site from the spike glycoprotein. *Genome Med* *12*, 68. [10.1186/s13073-020-00763-0](https://doi.org/10.1186/s13073-020-00763-0).

Elbe, S., and Buckland-Merrett, G. (2017). Data, disease and diplomacy: GISAID's innovative contribution to global health. *Glob Chall* *1*, 33-46. [10.1002/gch2.1018](https://doi.org/10.1002/gch2.1018).

Glowacka, I., Bertram, S., Muller, M.A., Allen, P., Soilleux, E., Pfefferle, S., Steffen, I., Tsegaye, T.S., He, Y., Gnirss, K., et al. (2011). Evidence that TMPRSS2 activates the severe acute respiratory syndrome coronavirus spike protein for membrane fusion and reduces viral control by the humoral immune response. *J Virol* *85*, 4122-4134. [10.1128/JVI.02232-10](https://doi.org/10.1128/JVI.02232-10).

Goettig, P., Brandstetter, H., and Magdolen, V. (2019). Surface loops of trypsin-like serine proteases as determinants of function. *Biochimie* *166*, 52-76. [10.1016/j.biochi.2019.09.004](https://doi.org/10.1016/j.biochi.2019.09.004).

Greaney, A.J., Loes, A.N., Crawford, K.H.D., Starr, T.N., Malone, K.D., Chu, H.Y., and Bloom, J.D. (2021a). Comprehensive mapping of mutations in the SARS-CoV-2 receptor-binding domain that affect recognition by polyclonal human plasma antibodies. *Cell Host Microbe* *29*, 463-476 e466. [10.1016/j.chom.2021.02.003](https://doi.org/10.1016/j.chom.2021.02.003).

Greaney, A.J., Starr, T.N., Gilchuk, P., Zost, S.J., Binshtein, E., Loes, A.N., Hilton, S.K., Huddleston, J., Eguia, R., Crawford, K.H.D., et al. (2021b). Complete Mapping of Mutations to the SARS-CoV-2 Spike Receptor-Binding Domain that Escape Antibody Recognition. *Cell Host Microbe* *29*, 44-57 e49. [10.1016/j.chom.2020.11.007](https://doi.org/10.1016/j.chom.2020.11.007).

378 Griffin, D.O., Brennan-Rieder, D., Ngo, B., Kory, P., Confalonieri, M., Shapiro, L., Iglesias, J.,  
379 Dube, M., Nanda, N., In, G.K., et al. (2021). The Importance of Understanding the Stages of  
380 COVID-19 in Treatment and Trials. *AIDS Rev.* 10.24875/AIDSRev.200001261.  
381 Hadfield, J., Megill, C., Bell, S.M., Huddleston, J., Potter, B., Callender, C., Sagulenko, P.,  
382 Bedford, T., and Neher, R.A. (2018). Nextstrain: real-time tracking of pathogen evolution.  
383 *Bioinformatics* 34, 4121-4123. 10.1093/bioinformatics/bty407.  
384 Hammond, J., Leister-Tebbe, H., Gardner, A., Abreu, P., Bao, W., Wisemandle, W., Baniecki,  
385 M., Hendrick, V.M., Damle, B., Simon-Campos, A., et al. (2022). Oral Nirmatrelvir for High-Risk,  
386 Nonhospitalized Adults with Covid-19. *N Engl J Med* 386, 1397-1408.  
387 10.1056/NEJMoa2118542.  
388 Harvey, W.T., Carabelli, A.M., Jackson, B., Gupta, R.K., Thomson, E.C., Harrison, E.M.,  
389 Ludden, C., Reeve, R., Rambaut, A., Consortium, C.-G.U., et al. (2021). SARS-CoV-2 variants,  
390 spike mutations and immune escape. *Nat Rev Microbiol* 19, 409-424. 10.1038/s41579-021-  
391 00573-0.  
392 Hekman, R.M., Hume, A.J., Goel, R.K., Abo, K.M., Huang, J., Blum, B.C., Werder, R.B., Suder,  
393 E.L., Paul, I., Phanse, S., et al. (2020). Actionable Cytopathogenic Host Responses of Human  
394 Alveolar Type 2 Cells to SARS-CoV-2. *Mol Cell* 80, 1104-1122 e1109.  
395 10.1016/j.molcel.2020.11.028.  
396 Hoffmann, M., Kleine-Weber, H., Schroeder, S., Kruger, N., Herrler, T., Erichsen, S.,  
397 Schiergens, T.S., Herrler, G., Wu, N.H., Nitsche, A., et al. (2020a). SARS-CoV-2 Cell Entry  
398 Depends on ACE2 and TMPRSS2 and Is Blocked by a Clinically Proven Protease Inhibitor. *Cell*  
399 181, 271-280 e278. 10.1016/j.cell.2020.02.052.  
400 Hoffmann, M., Schroeder, S., Kleine-Weber, H., Muller, M.A., Drosten, C., and Pohlmann, S.  
401 (2020b). Nafamostat Mesylate Blocks Activation of SARS-CoV-2: New Treatment Option for  
402 COVID-19. *Antimicrob Agents Chemother* 64. 10.1128/AAC.00754-20.  
403 Hou, Y.J., Chiba, S., Halfmann, P., Ehre, C., Kuroda, M., Dinno, K.H., 3rd, Leist, S.R., Schafer,  
404 A., Nakajima, N., Takahashi, K., et al. (2020). SARS-CoV-2 D614G variant exhibits efficient  
405 replication ex vivo and transmission in vivo. *Science* 370, 1464-1468.  
406 10.1126/science.abe8499.  
407 Jaimes, J., Millet, J., and Whittaker, G. (2020a). Proteolytic Cleavage of the SARS-CoV-2 Spike  
408 Protein and the Role of the Novel S1/S2 Site. SSRN, 3581359. 10.2139/ssrn.3581359.  
409 Jaimes, J.A., Andre, N.M., Chappie, J.S., Millet, J.K., and Whittaker, G.R. (2020b). Phylogenetic  
410 Analysis and Structural Modeling of SARS-CoV-2 Spike Protein Reveals an Evolutionary  
411 Distinct and Proteolytically Sensitive Activation Loop. *J Mol Biol* 432, 3309-3325.  
412 10.1016/j.jmb.2020.04.009.  
413 Jaimes, J.A., Millet, J.K., and Whittaker, G.R. (2020c). Proteolytic Cleavage of the SARS-CoV-2  
414 Spike Protein and the Role of the Novel S1/S2 Site. *iScience* 23, 101212.  
415 10.1016/j.isci.2020.101212.  
416 Kastenhuber, E.R., Mercadante, M., Nilsson-Payant, B., Johnson, J.L., Jaimes, J.A., Muecksch,  
417 F., Weisblum, Y., Bram, Y., Chandar, V., Whittaker, G.R., et al. (2022). Coagulation factors  
418 directly cleave SARS-CoV-2 spike and enhance viral entry. *Elife* 11. 10.7554/eLife.77444.  
419 Kim, Y.I., Kim, S.G., Kim, S.M., Kim, E.H., Park, S.J., Yu, K.M., Chang, J.H., Kim, E.J., Lee, S.,  
420 Casel, M.A.B., et al. (2020). Infection and Rapid Transmission of SARS-CoV-2 in Ferrets. *Cell*  
421 Host Microbe 27, 704-709 e702. 10.1016/j.chom.2020.03.023.  
422 Kistler, K.E., Huddleston, J., and Bedford, T. (2021). Rapid and parallel adaptive mutations in  
423 spike S1 drive clade success in SARS-CoV-2. *bioRxiv*. 10.1101/2021.09.11.459844.  
424 Klann, K., Bojkova, D., Tascher, G., Ciesek, S., Munch, C., and Cinatl, J. (2020). Growth Factor  
425 Receptor Signaling Inhibition Prevents SARS-CoV-2 Replication. *Mol Cell* 80, 164-174 e164.  
426 10.1016/j.molcel.2020.08.006.

427 Konings, F., Perkins, M.D., Kuhn, J.H., Pallen, M.J., Alm, E.J., Archer, B.N., Barakat, A.,  
428 Bedford, T., Bhiman, J.N., Caly, L., et al. (2021). SARS-CoV-2 Variants of Interest and Concern  
429 naming scheme conducive for global discourse. *Nat Microbiol* 6, 821-823. 10.1038/s41564-021-  
430 00932-w.

431 Korber, B., Fischer, W.M., Gnanakaran, S., Yoon, H., Theiler, J., Abfalterer, W., Hengartner, N.,  
432 Giorgi, E.E., Bhattacharya, T., Foley, B., et al. (2020). Tracking Changes in SARS-CoV-2 Spike:  
433 Evidence that D614G Increases Infectivity of the COVID-19 Virus. *Cell* 182, 812-827 e819.  
434 10.1016/j.cell.2020.06.043.

435 Kumar, S., Tao, Q., Weaver, S., Sanderford, M., Caraballo-Ortiz, M.A., Sharma, S., Pond,  
436 S.L.K., and Miura, S. (2021). An Evolutionary Portrait of the Progenitor SARS-CoV-2 and Its  
437 Dominant Offshoots in COVID-19 Pandemic. *Mol Biol Evol* 38, 3046-3059.  
438 10.1093/molbev/msab118.

439 Leist, S.R., Dinnon, K.H., 3rd, Schafer, A., Tse, L.V., Okuda, K., Hou, Y.J., West, A., Edwards,  
440 C.E., Sanders, W., Fritch, E.J., et al. (2020). A Mouse-Adapted SARS-CoV-2 Induces Acute  
441 Lung Injury and Mortality in Standard Laboratory Mice. *Cell* 183, 1070-1085 e1012.  
442 10.1016/j.cell.2020.09.050.

443 Letko, M., Marzi, A., and Munster, V. (2020). Functional assessment of cell entry and receptor  
444 usage for SARS-CoV-2 and other lineage B betacoronaviruses. *Nat Microbiol* 5, 562-569.  
445 10.1038/s41564-020-0688-y.

446 Li, K., Meyerholz, D.K., Bartlett, J.A., and McCray, P.B., Jr. (2021). The TMPRSS2 Inhibitor  
447 Nafamostat Reduces SARS-CoV-2 Pulmonary Infection in Mouse Models of COVID-19. *mBio*  
448 12, e0097021. 10.1128/mBio.00970-21.

449 Liu, Y., Liu, J., Johnson, B.A., Xia, H., Ku, Z., Schindewolf, C., Widen, S.G., An, Z., Weaver,  
450 S.C., Menachery, V.D., et al. (2021). Delta spike P681R mutation enhances SARS-CoV-2  
451 fitness over Alpha variant. *bioRxiv*. 10.1101/2021.08.12.456173.

452 Lubinski, B., Frazier, L.E., M, V.T.P., Bugembe, D.L., Tang, T., Daniel, S., Cotten, M., Jaimes,  
453 J.A., and Whittaker, G.R. (2021a). Spike protein cleavage-activation mediated by the SARS-  
454 CoV-2 P681R mutation: a case-study from its first appearance in variant of interest (VOI) A.23.1  
455 identified in Uganda. *bioRxiv*. 10.1101/2021.06.30.450632.

456 Lubinski, B., Tang, T., Daniel, S., Jaimes, J.A., and Whittaker, G.R. (2021b). Functional  
457 evaluation of proteolytic activation for the SARS-CoV-2 variant B.1.1.7: role of the P681H  
458 mutation. *bioRxiv*. 10.1101/2021.04.06.438731.

459 Maxmen, A., and Mallapaty, S. (2021). The COVID lab-leak hypothesis: what scientists do and  
460 don't know. *Nature* 594, 313-315. 10.1038/d41586-021-01529-3.

461 McNamara, L.A., Wiegand, R.E., Burke, R.M., Sharma, A.J., Sheppard, M., Adjemian, J.,  
462 Ahmad, F.B., Anderson, R.N., Barbour, K.E., Binder, A.M., et al. (2022). Estimating the early  
463 impact of the US COVID-19 vaccination programme on COVID-19 cases, emergency  
464 department visits, hospital admissions, and deaths among adults aged 65 years and older: an  
465 ecological analysis of national surveillance data. *Lancet* 399, 152-160. 10.1016/S0140-  
466 6736(21)02226-1.

467 Menachery, V.D., Dinnon, K.H., 3rd, Yount, B.L., Jr., McAnarney, E.T., Gralinski, L.E., Hale, A.,  
468 Graham, R.L., Scobey, T., Anthony, S.J., Wang, L., et al. (2020). Trypsin Treatment Unlocks  
469 Barrier for Zoonotic Bat Coronavirus Infection. *J Virol* 94. 10.1128/JVI.01774-19.

470 Meredith, L.W., Hamilton, W.L., Warne, B., Houldcroft, C.J., Hosmillo, M., Jahun, A.S., Curran,  
471 M.D., Parmar, S., Caller, L.G., Caddy, S.L., et al. (2020). Rapid implementation of SARS-CoV-2  
472 sequencing to investigate cases of health-care associated COVID-19: a prospective genomic  
473 surveillance study. *Lancet Infect Dis* 20, 1263-1272. 10.1016/S1473-3099(20)30562-4.

474 Mesle, M.M., Brown, J., Mook, P., Hagan, J., Pastore, R., Bundle, N., Spiteri, G., Ravasi, G.,  
475 Nicolay, N., Andrews, N., et al. (2021). Estimated number of deaths directly averted in people

476 60 years and older as a result of COVID-19 vaccination in the WHO European Region,  
477 December 2020 to November 2021. *Euro Surveill* 26. 10.2807/1560-  
478 7917.ES.2021.26.47.2101021.  
479 Millet, J.K., and Whittaker, G.R. (2014). Host cell entry of Middle East respiratory syndrome  
480 coronavirus after two-step, furin-mediated activation of the spike protein. *Proc Natl Acad Sci U S*  
481 *A* 111, 15214-15219. 10.1073/pnas.1407087111.  
482 Mlcochova, P., Kemp, S., Dhar, M.S., Papa, G., Meng, B., Ferreira, I., Datir, R., Collier, D.A.,  
483 Albecka, A., Singh, S., et al. (2021). SARS-CoV-2 B.1.617.2 Delta variant replication and  
484 immune evasion. *Nature*. 10.1038/s41586-021-03944-y.  
485 Niemeyer, B.F., Miller, C.M., Ledesma-Feliciano, C., Morrison, J.H., Jimenez-Valdes, R., Clifton,  
486 C., Poeschla, E.M., and Benam, K.H. (2021). Broad antiviral and anti-inflammatory efficacy of  
487 nafamostat against SARS-CoV-2 and seasonal coronaviruses in primary human bronchiolar  
488 epithelia. *Nano Sel.* 10.1002/nano.202100123.  
489 Ord, M., Faustova, I., and Loog, M. (2020). The sequence at Spike S1/S2 site enables cleavage  
490 by furin and phospho-regulation in SARS-CoV2 but not in SARS-CoV1 or MERS-CoV. *Sci Rep*  
491 10, 16944. 10.1038/s41598-020-74101-0.  
492 Ou, X., Liu, Y., Lei, X., Li, P., Mi, D., Ren, L., Guo, L., Guo, R., Chen, T., Hu, J., et al. (2020).  
493 Characterization of spike glycoprotein of SARS-CoV-2 on virus entry and its immune cross-  
494 reactivity with SARS-CoV. *Nat Commun* 11, 1620. 10.1038/s41467-020-15562-9.  
495 Planas, D., Saunders, N., Maes, P., Guivel-Benhassine, F., Planchais, C., Buchrieser, J.,  
496 Bolland, W.H., Porrot, F., Staropoli, I., Lemoine, F., et al. (2022). Considerable escape of  
497 SARS-CoV-2 Omicron to antibody neutralization. *Nature* 602, 671-675. 10.1038/s41586-021-  
498 04389-z.  
499 Plante, J.A., Liu, Y., Liu, J., Xia, H., Johnson, B.A., Lokugamage, K.G., Zhang, X., Muruato,  
500 A.E., Zou, J., Fontes-Garfias, C.R., et al. (2021). Spike mutation D614G alters SARS-CoV-2  
501 fitness. *Nature* 592, 116-121. 10.1038/s41586-020-2895-3.  
502 Puente, X.S., Gutierrez-Fernandez, A., Ordonez, G.R., Hillier, L.W., and Lopez-Otin, C. (2005).  
503 Comparative genomic analysis of human and chimpanzee proteases. *Genomics* 86, 638-647.  
504 10.1016/j.ygeno.2005.07.009.  
505 Quinn, T.M., Gaughan, E.E., Bruce, A., Antonelli, J., O'Connor, R., Li, F., McNamara, S., Koch,  
506 O., MacKintosh, C., Dockrell, D., et al. (2022). Randomised controlled trial of intravenous  
507 nafamostat mesylate in COVID pneumonitis: Phase 1b/2a experimental study to investigate  
508 safety, Pharmacokinetics and Pharmacodynamics. *EBioMedicine* 76, 103856.  
509 10.1016/j.ebiom.2022.103856.  
510 Rawlings, N.D., Barrett, A.J., Thomas, P.D., Huang, X., Bateman, A., and Finn, R.D. (2018).  
511 The MEROPS database of proteolytic enzymes, their substrates and inhibitors in 2017 and a  
512 comparison with peptidases in the PANTHER database. *Nucleic Acids Res* 46, D624-D632.  
513 10.1093/nar/gkx1134.  
514 Sagulenko, P., Puller, V., and Neher, R.A. (2018). TreeTime: Maximum-likelihood phylodynamic  
515 analysis. *Virus Evol* 4, vex042. 10.1093/ve/vex042.  
516 Shapira, T., Monreal, I.A., Dion, S.P., Buchholz, D.W., Imbiakha, B., Olmstead, A.D., Jager, M.,  
517 Desilets, A., Gao, G., Martins, M., et al. (2022). A TMPRSS2 inhibitor acts as a pan-SARS-CoV-  
518 2 prophylactic and therapeutic. *Nature* 605, 340-348. 10.1038/s41586-022-04661-w.  
519 Shuai, H., Chan, J.F., Hu, B., Chai, Y., Yuen, T.T., Yin, F., Huang, X., Yoon, C., Hu, J.C., Liu,  
520 H., et al. (2022). Attenuated replication and pathogenicity of SARS-CoV-2 B.1.1.529 Omicron.  
521 *Nature* 603, 693-699. 10.1038/s41586-022-04442-5.  
522 Sia, S.F., Yan, L.M., Chin, A.W.H., Fung, K., Choy, K.T., Wong, A.Y.L., Kaewpreedee, P.,  
523 Perera, R., Poon, L.L.M., Nicholls, J.M., et al. (2020). Pathogenesis and transmission of SARS-  
524 CoV-2 in golden hamsters. *Nature* 583, 834-838. 10.1038/s41586-020-2342-5.

525 Starr, T.N., Greaney, A.J., Addetia, A., Hannon, W.W., Choudhary, M.C., Dingens, A.S., Li, J.Z.,  
526 and Bloom, J.D. (2021). Prospective mapping of viral mutations that escape antibodies used to  
527 treat COVID-19. *Science* 371, 850-854. 10.1126/science.abf9302.

528 Starr, T.N., Greaney, A.J., Hilton, S.K., Ellis, D., Crawford, K.H.D., Dingens, A.S., Navarro, M.J.,  
529 Bowen, J.E., Tortorici, M.A., Walls, A.C., et al. (2020). Deep Mutational Scanning of SARS-CoV-  
530 2 Receptor Binding Domain Reveals Constraints on Folding and ACE2 Binding. *Cell* 182, 1295-  
531 1310 e1220. 10.1016/j.cell.2020.08.012.

532 Stukalov, A., Girault, V., Grass, V., Karayel, O., Bergant, V., Urban, C., Haas, D.A., Huang, Y.,  
533 Oubraham, L., Wang, A., et al. (2021). Multilevel proteomics reveals host perturbations by  
534 SARS-CoV-2 and SARS-CoV. *Nature* 594, 246-252. 10.1038/s41586-021-03493-4.

535 Tang, T., Jaimes, J.A., Bidon, M.K., Straus, M.R., Daniel, S., and Whittaker, G.R. (2021).  
536 Proteolytic Activation of SARS-CoV-2 Spike at the S1/S2 Boundary: Potential Role of Proteases  
537 beyond Furin. *ACS Infect Dis* 7, 264-272. 10.1021/acscinfecdis.0c00701.

538 Ulrich, L., Halwe, N.J., Taddeo, A., Ebert, N., Schon, J., Devisme, C., Trueb, B.S., Hoffmann,  
539 B., Wider, M., Fan, X., et al. (2022). Enhanced fitness of SARS-CoV-2 variant of concern Alpha  
540 but not Beta. *Nature* 602, 307-313. 10.1038/s41586-021-04342-0.

541 Victora, P.C., Castro, P.M.C., Gurzenda, S., Medeiros, A.C., Franca, G.V.A., and Barros, P.  
542 (2021). Estimating the early impact of vaccination against COVID-19 on deaths among elderly  
543 people in Brazil: Analyses of routinely-collected data on vaccine coverage and mortality.  
544 *EClinicalMedicine* 38, 101036. 10.1016/j.eclinm.2021.101036.

545 Walensky, R.P., Walke, H.T., and Fauci, A.S. (2021). SARS-CoV-2 Variants of Concern in the  
546 United States-Challenges and Opportunities. *JAMA* 325, 1037-1038. 10.1001/jama.2021.2294.

547 Walls, A.C., Park, Y.J., Tortorici, M.A., Wall, A., McGuire, A.T., and Velesler, D. (2020).  
548 Structure, Function, and Antigenicity of the SARS-CoV-2 Spike Glycoprotein. *Cell* 181, 281-292  
549 e286. 10.1016/j.cell.2020.02.058.

550 Wang, P., Nair, M.S., Liu, L., Iketani, S., Luo, Y., Guo, Y., Wang, M., Yu, J., Zhang, B., Kwong,  
551 P.D., et al. (2021a). Antibody resistance of SARS-CoV-2 variants B.1.351 and B.1.1.7. *Nature*  
552 593, 130-135. 10.1038/s41586-021-03398-2.

553 Wang, Z., Schmidt, F., Weisblum, Y., Muecksch, F., Barnes, C.O., Finkin, S., Schaefer-  
554 Babajew, D., Cipolla, M., Gaebler, C., Lieberman, J.A., et al. (2021b). mRNA vaccine-elicited  
555 antibodies to SARS-CoV-2 and circulating variants. *Nature*. 10.1038/s41586-021-03324-6.

556 Weisblum, Y., Schmidt, F., Zhang, F., DaSilva, J., Poston, D., Lorenzi, J.C., Muecksch, F.,  
557 Rutkowska, M., Hoffmann, H.H., Michailidis, E., et al. (2020). Escape from neutralizing  
558 antibodies by SARS-CoV-2 spike protein variants. *Elife* 9. 10.7554/eLife.61312.

559 Wu, Y., and Zhao, S. (2020). Furin cleavage sites naturally occur in coronaviruses. *Stem Cell*  
560 *Res* 50, 102115. 10.1016/j.scr.2020.102115.

561 Yaron, T.M., Heaton, B.E., Levy, T.M., Johnson, J.L., Jordan, T.X., Cohen, B.M., Kerelsky, A.,  
562 Lin, T.Y., Liberatore, K.M., Bulaon, D.K., et al. (2020). The FDA-approved drug Alectinib  
563 compromises SARS-CoV-2 nucleocapsid phosphorylation and inhibits viral infection in vitro.  
564 *bioRxiv*. 10.1101/2020.08.14.251207.

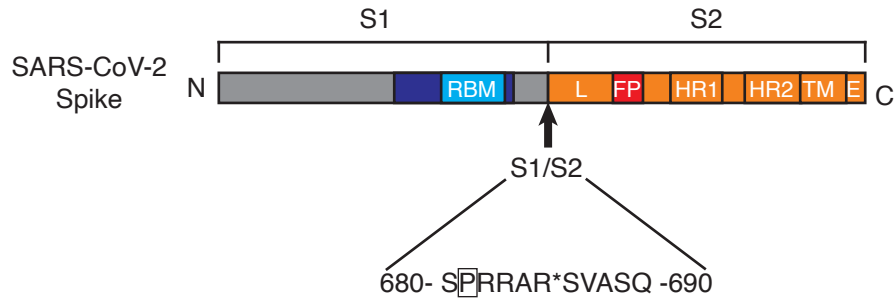
565 Zheng, J., Wong, L.R., Li, K., Verma, A.K., Ortiz, M.E., Wohlford-Lenane, C., Leidinger, M.R.,  
566 Knudson, C.M., Meyerholz, D.K., McCray, P.B., Jr., and Perlman, S. (2021). COVID-19  
567 treatments and pathogenesis including anosmia in K18-hACE2 mice. *Nature* 589, 603-607.  
568 10.1038/s41586-020-2943-z.

569 Zhou, B., Thao, T.T.N., Hoffmann, D., Taddeo, A., Ebert, N., Labroussaa, F., Pohlmann, A.,  
570 King, J., Steiner, S., Kelly, J.N., et al. (2021). SARS-CoV-2 spike D614G change enhances  
571 replication and transmission. *Nature* 592, 122-127. 10.1038/s41586-021-03361-1.

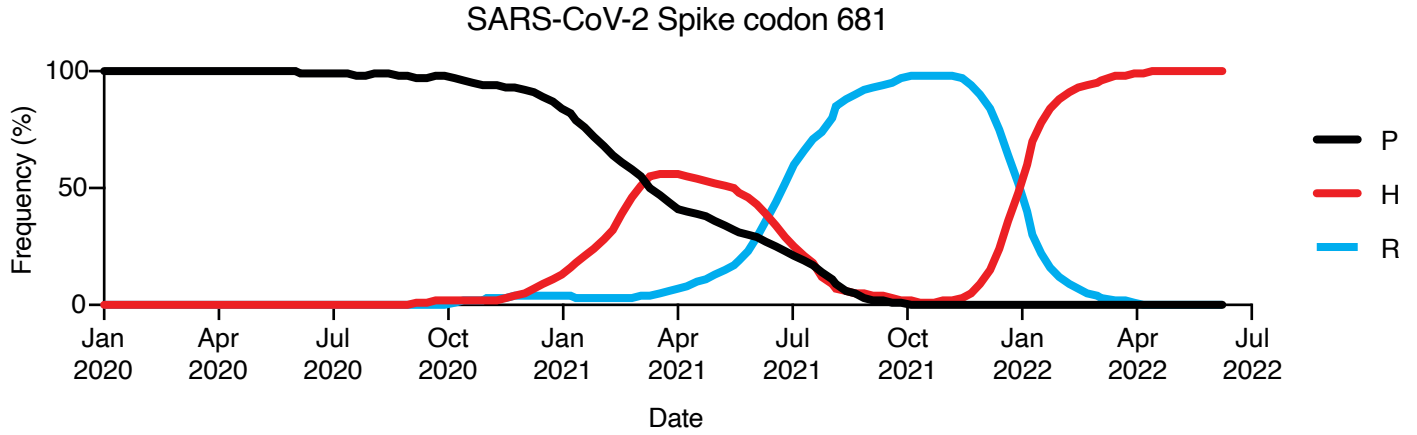
572

# Fig. 1. Sequence divergence of SARS-CoV-2 spike codon 681 among variants of concern

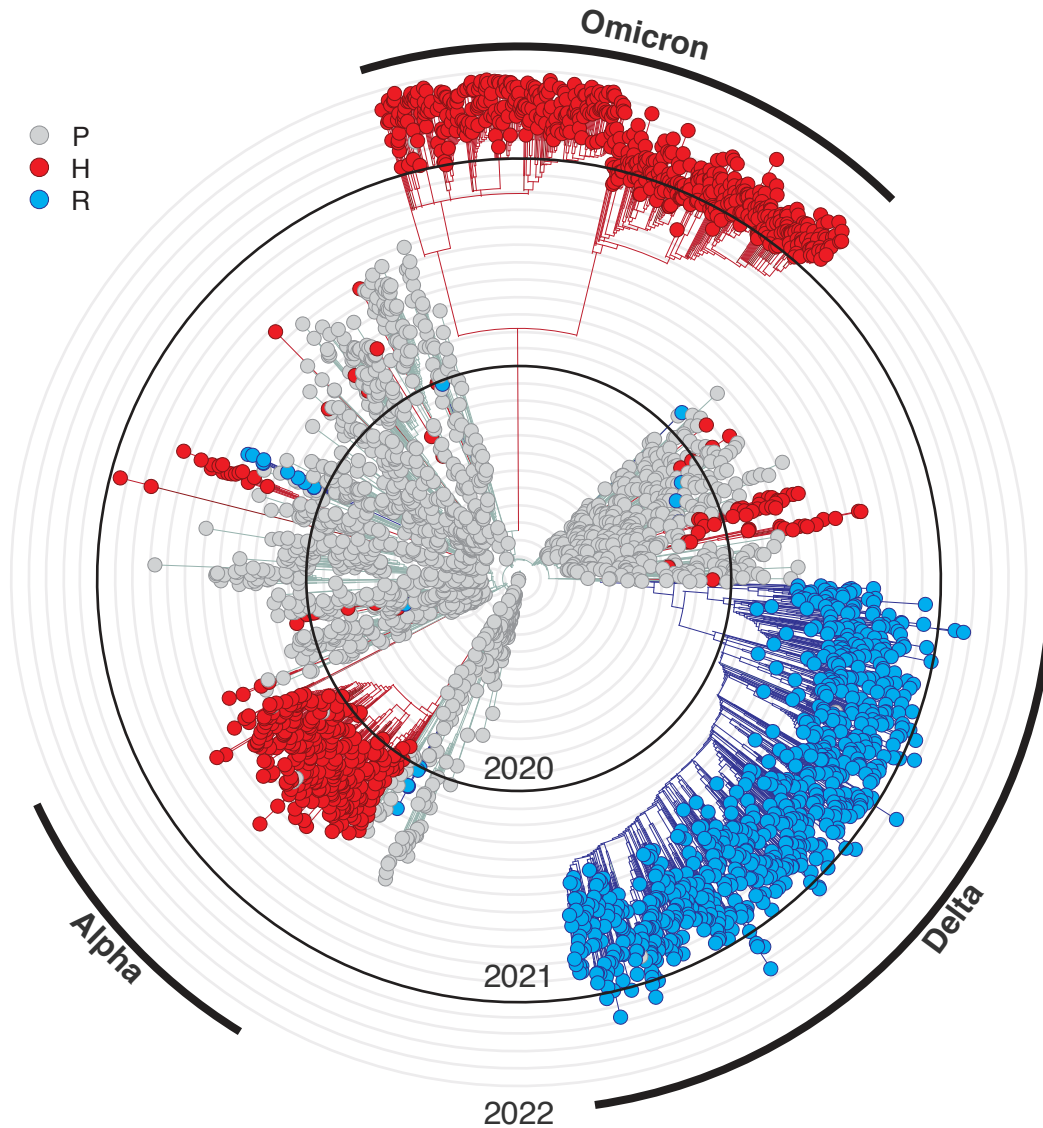
**A**



**B**

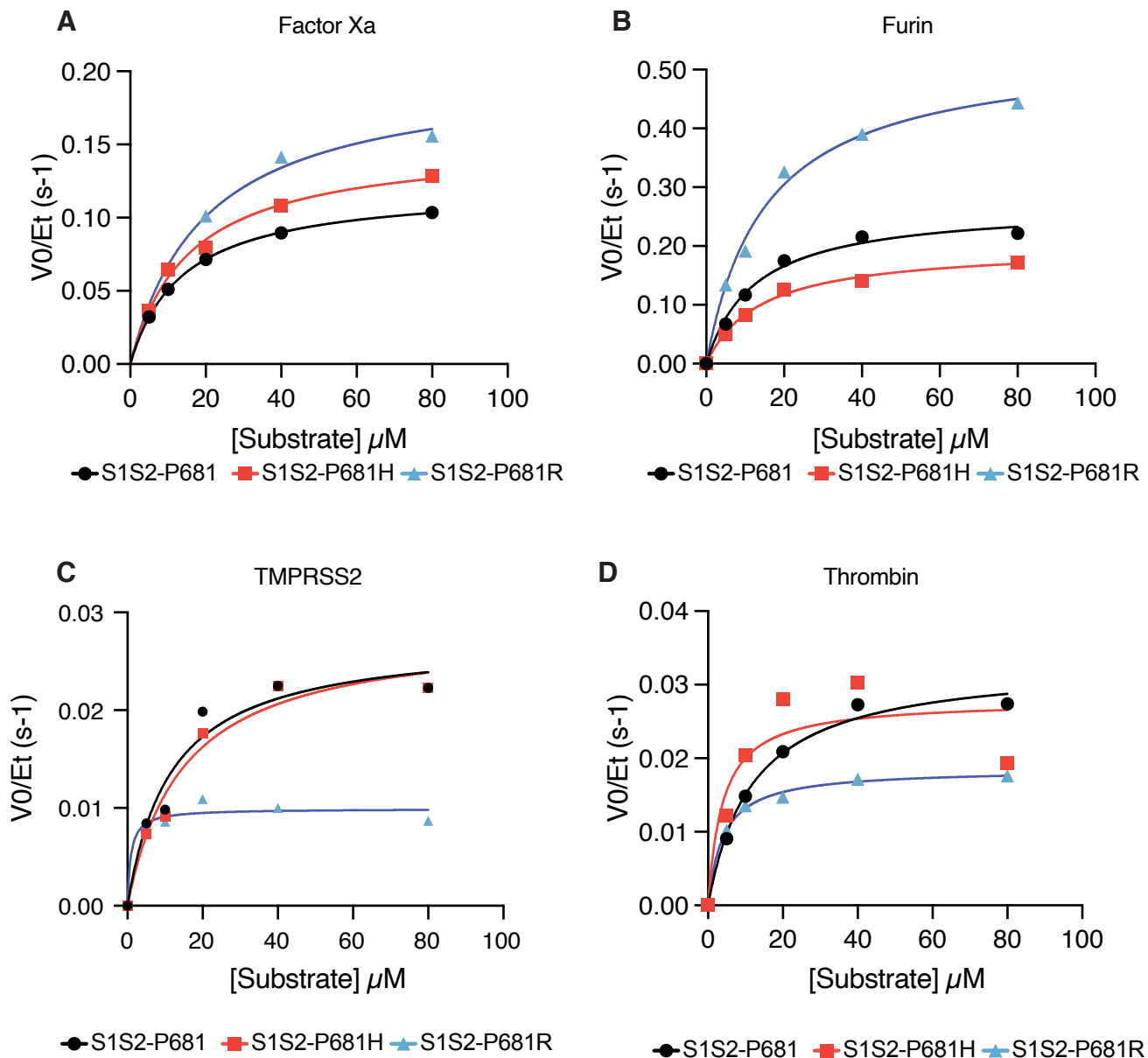


**C**





## Fig. 2. Substitutions at SARS-CoV-2 Spike S1/S2 site cause divergent changes to interactions with host proteases





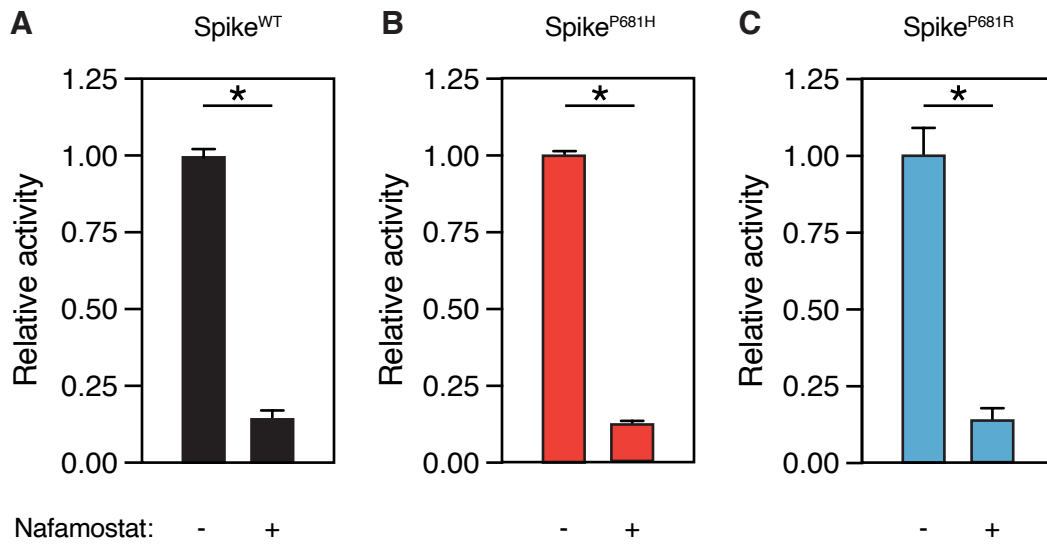


### Fig. 3. Factor Xa cleavage of SARS-CoV-2 variants remains sensitive to nafamostat



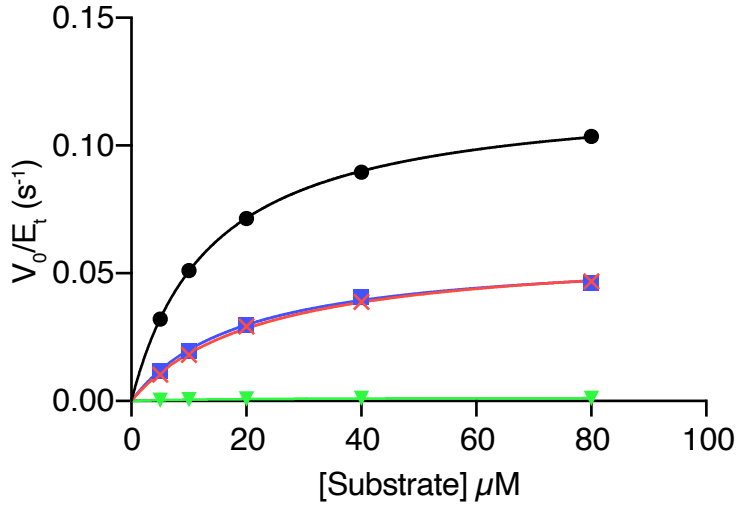
**Fig. 4. Effect of phosphorylation at the S1/S2 site on spike cleavage**

**A**

 S1S2 680- SPRRAR*SVASQ -690	 S1S2-p-S680 680- <sup>Ⓟ</sup> SPRRAR*SVASQ -690	 S1S2-p-S686 680- <sup>Ⓟ</sup> SPRRAR*SVASQ -690	 S1S2-p-S689 680- <sup>Ⓟ</sup> SPRRAR*SVASQ -690
--	--	--	--

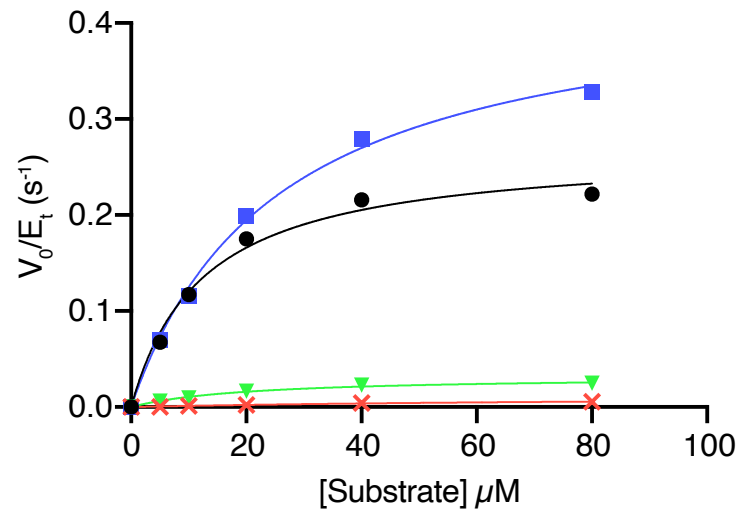
**B**

Factor Xa



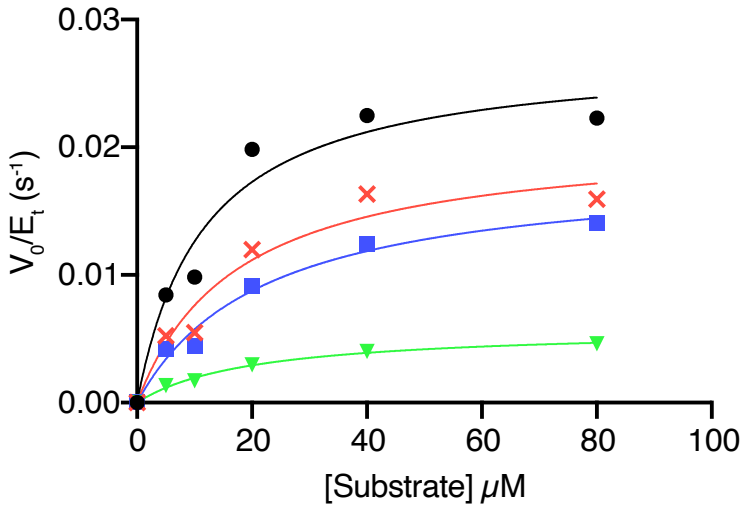
**C**

Furin



**D**

TMPRSS2



**E**

Thrombin

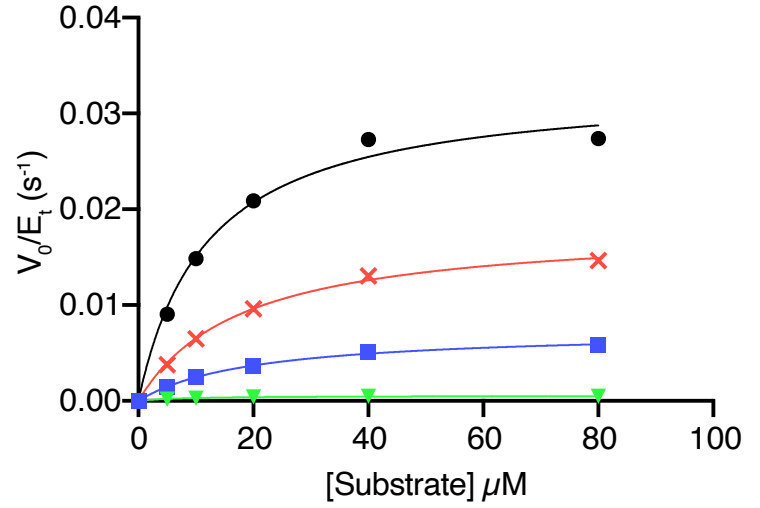


**Fig. 5. Proteolytic fingerprint of diverse coronavirus lineages.**

